

UNIVERSITÀ DEGLI STUDI DI PAVIA

SCIENTIFICA ACTA

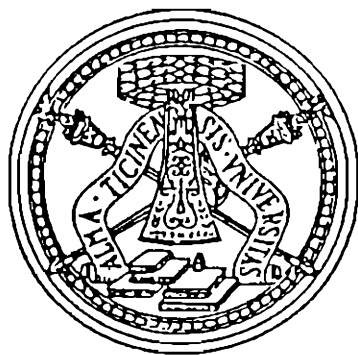
QUADERNI DEL DOTTORATO

VOLUME IV

ANNO IV

NUMERO 2

15 GIUGNO 1989



ISTITUTO NAZIONALE DI FISICA NUCLEARE

CENTRO STAMPA - DIPARTIMENTI FISICI
via Bassi, 6 27100 Pavia

INDICE

- 1 - SOLAR WIND AND PHYSICS OF THE HELIOSPHERE
B. Coppi pag. 2

- 2 - THE IGNITOR PROJECT
B. Coppi, F. Pegoraro pag. 32

Bruno Coppi

**Massachusetts Institute of Technology
Cambridge, Massachusetts 02139**

**SOLAR WIND AND PHYSICS
OF THE HELIOSPHERE**

Lezione inaugurale Anno Accademico 1985/86

1. INTRODUCTION

The possibility to carry out physics experiments by means of spacecraft that can sample significant portions of the solar system has led us to view this as a unique type of laboratory¹ in which, for instance, our theoretical understanding of rarefied plasmas² can be tested at the microscopic level while new phenomena continue to be discovered³. With this perspective, we present some of the more revealing experimental observations that have been made in the field of "near" space physics⁴ and of the theoretical problems that these observations have brought to our attention.

The heliosphere can be identified as the region of the galactic plasma that is affected by the solar system. We recall that the best known and, so far, most evident forms of influence of the Sun on its planets are the gravitational interaction that binds them and its typical emission of electromagnetic radiation (e.g. light and heat). In addition to these, we have recently become more deeply aware of the important role that the so-called solar wind, the persistent high velocity outflow of plasma from the Sun, plays in the solar system.

As the solar wind flows away from the Sun, it must eventually come under the influence of the particles and fields of the local interstellar medium⁵. In the neighborhood of the solar system, the interstellar medium has four main

components⁶ : a magnetic field (~ 3.5 microgauss), a thermal plasma, whose density n and temperature T are rather uncertain ($0.02 < n < 0.07 \text{ cm}^{-3}$, $10^3 < T < 10^4 \text{ }^\circ\text{K}$); a neutral gas with density $0.06 < n_g < 0.1 \text{ cm}^{-3}$ and temperature in the same range as that of the plasma; and cosmic rays with an energy density of about 1 eV cm^{-3} . The magnetized interstellar plasma will tend to interact with the magnetized solar wind plasma at a somewhat diffuse boundary, while the interstellar neutral gas and cosmic rays can penetrate deeply inside this boundary. The Sun's velocity relative to the interstellar medium is about $V_o \sim 20 \text{ km s}^{-1}$. Assuming that the relevant plasma may be treated as fluids (a fact that we shall dispute on the basis of "in situ" experimental observations), it is commonly argued that the condition for pressure balance at the heliosphere boundary, between the solar wind and interstellar plasma, requires subsonic solar wind flow inside the boundary and a shock transition somewhere upstream. The subsonic flow region can be expected to have a comet-like tail configuration as indicated in Fig. 1. The distance of the stagnation point on the eliosphere boundary from the Sun has been estimated roughly to be from 50 to 150 AU (AU = astronomical unit; $1\text{AU} = 1.5 \times 10^8 \text{ Km}$).

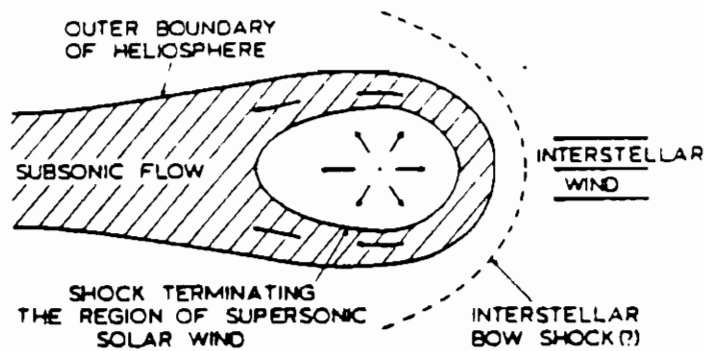


Figure 1: Schematic representation of the heliosphere. In the real heliosphere, none of the boundaries shown is likely to be either simple or fixed, owing to the structuring of the solar wind⁵.

The first direct measurements of the solar wind were performed by Bonetti, et al., ¹. Indirect evidence for the solar wind had accumulated over the years as recounted in Ref. [7], but in the fifties, Biermann ⁸ suggested that only a stream of particles originating from the Sun could account for the "pushing away" from the Sun of the tails of comets entering the solar system.

He also suggested that this form of "radiation" from the Sun would also account for the existence of excited, light emitting ions seen in comet tails.

As we shall see in the following sections, the magnetic configuration ⁹ that is typical of the solar wind in the ecliptic plane can be represented, roughly, by a spiral (Fig. 2). In fact, this can be regarded as the effect of having the solar magnetic field "carried" along by the stream of particles emanating from the Sun and is similar to the pattern of the water droplets produced by a rotating garden sprinkler. On average, at 1 AU the total thermal energy is only about 1 percent of the energy of the flow motion in the solar wind. The rate of

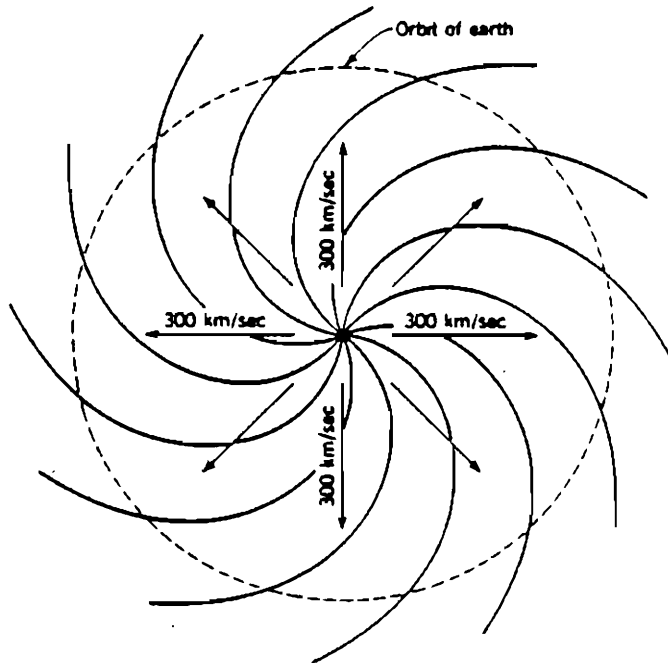


Figure 2: Model pattern of interplanetary magnetic field lines in the solar equatorial plane when a radial solar wind velocity of 300 km/sec is assumed⁹.

mass loss from the Sun by the solar wind is negligible as it correspond to a time of about 5×10^{13} years, but the rate of loss of angular momentum is significant and the relevant time [6] has been estimated to be about 7×10^9 years. In fact, this time is comparable with the expected time scale of thermonuclear evolution for the Sun and thus may have important consequences in the evolution of the solar system [6].

A large domain of the heliosphere ranging from 0.3 AU to 10 AU has been explored "in situ" and carefully analyzed in the proximity of the ecliptic

plane. However, the dependence of the solar wind parameters on the heliographic latitude (in particular, at angles larger than 16° from the ecliptic plane¹⁰ remains to be explored. We also have scarce information on the physics of the inner heliosphere, the region extending from the heart of the solar corona to a distance of about 60 solar radii from the Sun.

In the same way that the properties of the magnetosphere of the earth vary dramatically with geomagnetic latitude, so we expect those of the heliosphere to be quite different as we move in latitude away from the plane of the ecliptic.

This viewpoint, for example, is substantiated by the striking asymmetry seen in images of the solar corona in photographs of the Sun in eclipse. Other examples of unknowns in the physics of the heliosphere (see also Sect. 6) are:

- a) the processes involved in the propagation of energetic solar particles in the corona, and in the interplanetary space;
- b) the nature of cosmic ray transport processes;
- c) the dynamic and spatial characteristics of interplanetary dust particles in the inner heliosphere, and their origin ;
- d) the temperature, density, and bulk velocity of interstellar neutral gas in the vicinity of the solar system.

Two classes (short and long range) of spacecraft have been employed for the physical exploration of the solar wind:

- a) Earth satellites whose orbits extend considerably beyond the Earth's bow shock (e.g., Explorer, Vela, IMP satellites)
- b) deep space probes whose primary mission was the encounter with one or more of the Sun planets, (e.g., Mariner, Pioneer, Helios 1 and 2, Voyager I and II).

In particular, the first class supplied a large amount of information on the temporal behaviour of the solar wind within 1 AU, over 2 solar cycles. The second class has led to the identification of the radial profiles of macroscopic plasma parameters such as the particle density, the electron and proton temperatures, the bulk velocity, etc. In addition, the distribution of particles as a function of the magnitude and direction of their velocities have been measured. This has important implications that will be discussed in the next Section.

In order to explore the heliosphere and view the Sun over the full range of heliolatitudes (see Fig. 3) an International Solar Polar Mission (ISPM) had been conceived and planned. The ISPM mission¹¹ was to be undertaken jointly by the European (ESA) and U.S. (NASA) space agencies. According to its original planning the ISPM would have employed two spacecrafts to make simultaneous measurements in both hemispheres, there by achieving the

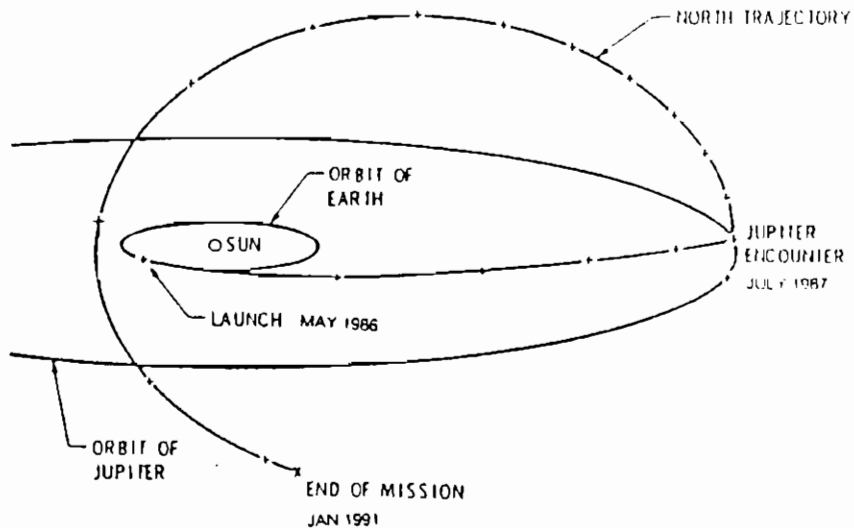


Figure 3: Typical trajectory overview¹¹ for the International Solar Polar Mission (ISPM). Note that because of continuing uncertainties concerning the ISPM launch configuration, the decision as to whether the initial post-Jupiter trajectory will be north- or south-bound has yet to be taken. Here only a north-bound trajectory is indicated.

"stereoscopic view" necessary for determining the three-dimensional properties of the inner heliosphere. However, in 1981 budget considerations led to the cancellation of the U.S. participation with the result that ISPM will have to rely on one spacecraft only (see Fig. 4). The scientific investigations on this spacecraft are expected to be started in 1986. A Jupiter (see Fig. 3) gravity-assist will be used to deflect the spacecraft into an elliptical orbit which¹² is inclined approximately at right-angle to the ecliptic plane.

Even before the first satellite observations became available, the existence of large scale structures in the solar wind usually termed "streams", had been inferred on the basis of observed variations in the Earth's magnetic field. In fact, recent observations have shown that there are several kinds of high-speed flows that might be called streams. Many of these seem to be contiguous or even superimposed on one another¹³. In the simplest cases, the solar wind velocity increases by several hundred kilometers per second over a period of one or two days and then decreases monotonically over two days. Compound streams show more complex variations of velocity with time

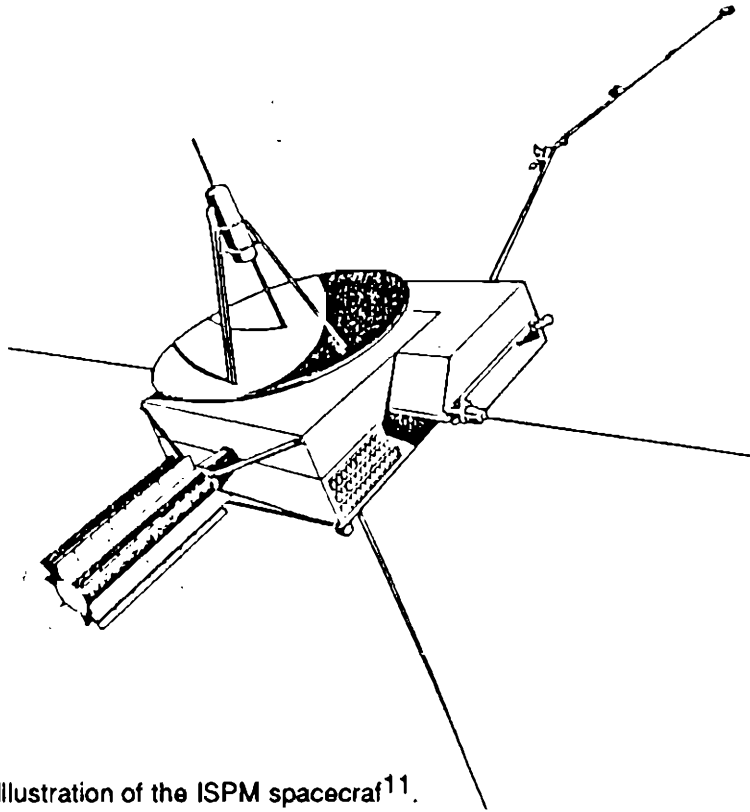


Figure 4: Illustration of the ISPM spacecraft¹¹.

and may be the result of the interaction of two or more simple streams. It is now believed¹⁴ that these recurrent streams originate from a relatively small number of localized regions of the Sun known as coronal holes. These regions of relatively low density and temperature are best seen in images¹⁵ of the Sun made at X-ray wavelengths (see Fig. 5).

Coronal holes were first observed at a time near the sunspot minimum. The holes around the poles seemed to be semipermanent; those at lower latitudes had lifetimes of several solar rotations. In recent years, during which sunspots have been approaching their maximum, the polar holes have become less prominent and the mean lifetime of the equatorial holes has decreased to only one or two rotations.

The identification of the origin and of the driving mechanism of the solar wind are two basic issues that are still unresolved. By the origin of the solar wind we mean where on the Sun the outflow of matter originates. This problem is intimately connected with understanding the nature of the solar

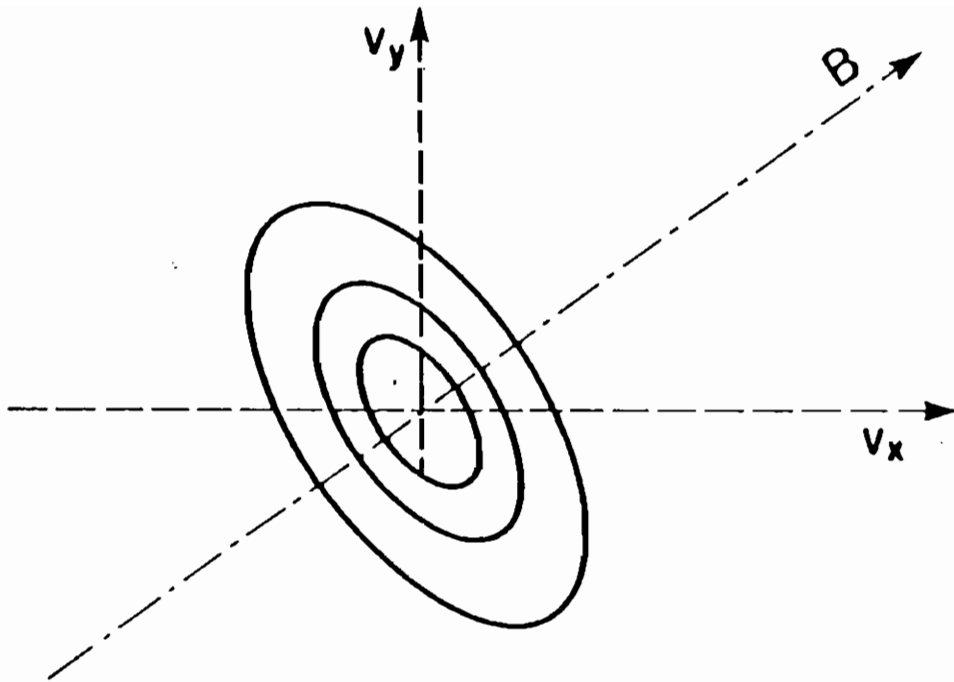


Figure 5: X-ray image of the Sun taken by the Skylab X-ray telescope on June 1973. This is a typical picture of the solar X-ray corona including a large meridional coronal hole in the center¹⁵.

corona that is still in a rudimentary stage¹⁶. The identification of a driving factor starts from assuming the presence and the heating of the solar corona as a given fact and implies understanding the processes that can maintain the observed particle outflow.

An important clue for this was in fact the discovery of the strong correlation between the high velocity streams of the solar wind and the open-line topology of the solar magnetic field above the coronal holes. Actually, no direct measurements have been made of the magnetic field in coronal holes, but observations of emission features in their vicinity suggest that the field is open and diverging¹⁷. It is generally assumed that the particle flow line and the field lines diverge rapidly above the hole¹⁸ and extend far into the corona. As may be deduced from X-ray images of the Sun, such as that in Fig. 5 and from photographs taken during eclipses, semipermanent holes are thought to exist at the north and south poles near sunspot minimum when the Sun's polar fields are strong.

Another clue may be offered by the discovery of persistent "suprathermal tails" in the distribution of electrons as a function of their velocities coupled with the characteristics of the proton, α -particle and other nuclei distributions that are described in the next section.

2. INADEQUACY OF FLUID-LIKE (AND THERMODYNAMIC) DESCRIPTIONS

As indicated by some of the remarks made in Section 1, the most immediate and rudimentary form of description for the heliosphere and the solar wind in particular is to treat them as fluid-like entities and to characterize them by quantities such as pressure and temperature that come from classical thermodynamics. The validity of this type of description is related to having particle distributions, as a function of velocity, that are close to a Maxwellian. We recall⁽²⁾ that this is expressed by

$$(1) \quad f_m = \frac{n}{(2\pi T/m)^{3/2}} \exp \left(-\frac{m}{2T} v^2 \right)$$

where v is the particle velocity measured in the frame of reference moving with the bulk (flow) velocity V of the medium (e.g., solar wind) that is being considered, n is the density, T the temperature and m the particle mass. Thus only one parameter, the temperature, is sufficient to identify the distribution in this case.

In particular the validity of a fluid-like description requires that the particle collision mean free path be shorter than the characteristic distances involved in the problem under consideration. In the case of the solar wind the collision mean free path is, roughly, of the order of 1 AU.

In the presence of a significant magnetic field the simplest distribution that takes into account the anisotropy of the plasma imbedded in this field, relative to its direction, is represented analytically by

$$(2) \quad f = \frac{n}{(2\pi T_{\perp}/m) (2\pi T_{\parallel}/m)^{1/2}} \exp \left\{ -\frac{m}{2} \left(\frac{v_{\perp}^2}{T_{\perp}} + \frac{v_{\parallel}^2}{T_{\parallel}} \right) \right\}$$

where v_{\parallel} is the parallel component and v_{\perp} the transverse component to the magnetic field of the particle velocity. The level curves of this function, corresponding to $f=\text{constant}$, are indicated in Fig. 6 for the case where $T_{\perp} > T_{\parallel}$. If $T_{\perp} = T_{\parallel}$, corresponding to Eq.(1), the level curves would be concentric

circles instead of ellipses. Notice that both distributions (1) and (2) have rotational symmetry about a line that is parallel to the direction of the magnetic field. This property is called gyrotropy.

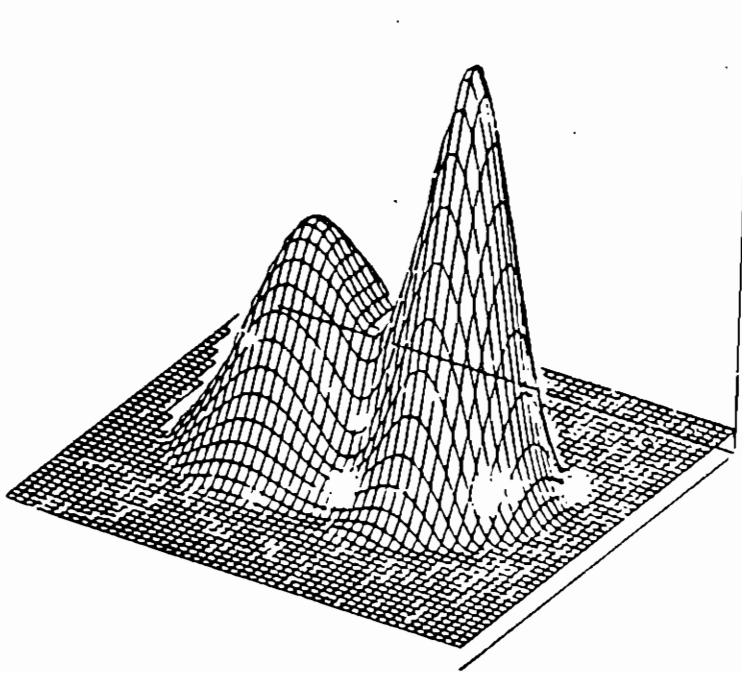


Figure 6: Level lines of a "bi-Maxwellian" two-temperature distribution function.

Thus one of the most basic experimental results obtained by the various spacecraft that have been employed to investigate the solar wind has been to obtain in situ measurements of the particle distributions. We refer first to the ion distributions and notice that all those measured by the Voyager spacecraft are gyrotropic relative to the magnetic field direction at the time of measurement¹⁹.

On the other hand, as we can expect in a plasma that, like the solar wind, is practically collisionless, a large variety of ion distributions has been observed. A sample of these is given in Fig. 7 obtained from the Helios spacecraft measurements²⁰. While distributions (1) and (2) have a single peak, we can see that the distributions represented in Fig. 7, except one, have a double peak. In order to illustrate this point further, a three-dimensional representation of a distribution of the same kind, that has been deduced from data obtained by the Voyager spacecraft²¹ is given in Fig. 8.

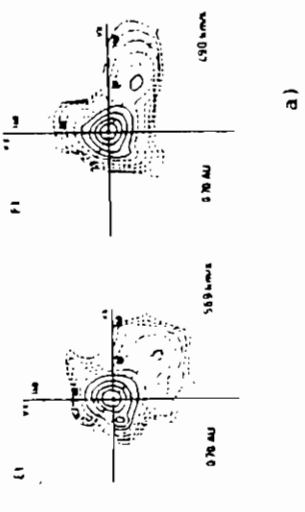
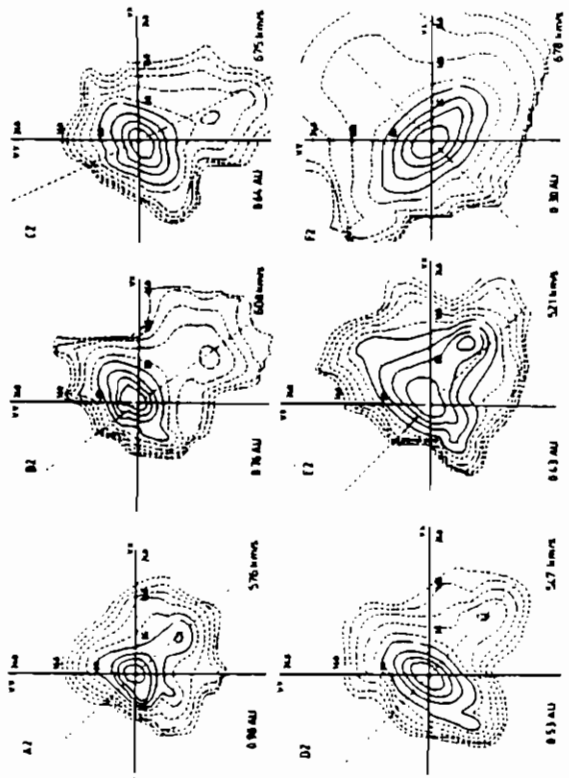


Figure 7: Experimental evidence of proton distributions measured as a function of particle velocity, that cannot be represented by a Maxwellian function [Eq. (1)]. Here level-lines of the proton distributions, obtained from the plasma detector onboard the Helios-2 spacecraft²⁰ for various heliocentric distances, are shown. The indicated particle velocities v_x and v_y are measured in the frame of reference solar wind with the solar wind refers to low and intermediate solar wind speed and exhibits a second component drifting along the magnetic field. Figure 7b shows intermediate and high speed proton distributions.

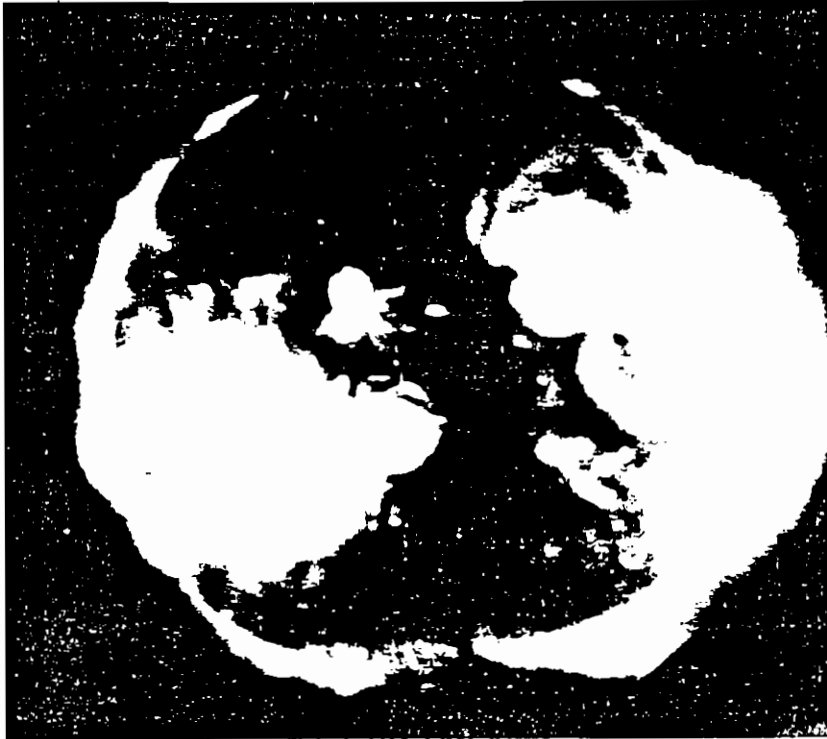


Figure 8: Three-dimensional representation of a non-Maxwellian proton distribution, in the frame of reference moving with the solar wind, measured by the M.I.T. plasma detector onboard the Voyager spacecraft²¹.

In addition to these representative cases there are others with intermediate features such as those with the region between the two peaks "filled up" to different degrees. In particular Fig. 7 shows the evidence of gyrotropy, that is of symmetry of the distribution around the indicated (by a dashed straight line) direction of the magnetic field and the considerable excess of T_{\perp} over T_{\parallel} for high velocity streams. These so-called "laterally extended" distributions are found more often near the Sun and may be considered as an indication of the existence of a specific mechanism for the increase of the average particle energy across the magnetic field. Experiments carried out in laboratory plasma can suggest appropriate processes for this, such as the excitation of certain plasma waves called lower hybrid modes (see Ref.[22]). On the other hand no serious attempt has been made so far to provide an explanation for the appearance of double-hump distributions such as those shown in Figs. 7 and 8.

Next to protons, α -particles, that is He^4 nuclei, are the most important components of the ion populations and correspond to few percent of the positive charge content. These particles have distributions, as a function of their velocities, with a wide variety of features as in the case of the proton distributions. In particular, α -particles generally have higher temperatures, a smaller value of T_{\perp}/T_{\parallel} and, at times, a drift velocity, relative to that of the protons, along the magnetic field¹⁰.

Thus it is clear, that a fluid-like description of the solar wind is indeed inadequate. In fact the strong reservations that we had expressed, before these revealing experimental data became available, on the extensive usage that had been made of this type of description, as well as of a spherical model for the geometrical configuration of the solar wind, were justified.

Then we consider the case of the measured electron distributions as a function of their velocity. For this we refer to a typical sample of the observed electron distributions, as reported in Ref.[23], that were obtained by the detectors on board the IMP-8 spacecraft during steady state conditions at 1 AU. These distribution functions have a strong skewed forward tail, away from the Sun, along the lines of the interplanetary magnetic field and this has been seen to be a permanent feature throughout a considerable portion of the explored solar system. In different terms, in the reference frame moving with the solar wind there are several times as many suprathermal electrons moving away from the Sun as toward the Sun.

A simple representation of these distributions is given in Fig. 9 as a

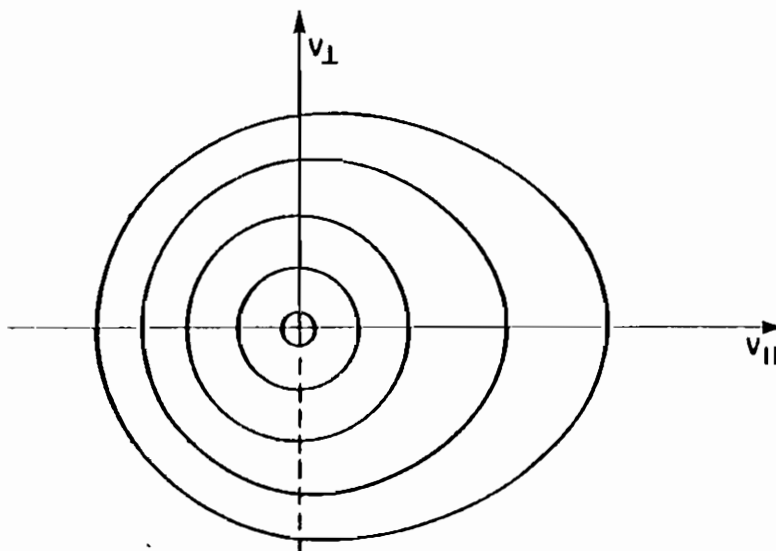


Figure 9: Level-lines of a type of electron distribution that can represent those measured in the solar wind.

combination of a "core" distribution that is a Maxwellian [see Eq.(1)] characterized by the density n_c and the temperature T_c , that refers to the thermal and subthermal electrons, and of a "fast" distribution f_F that refers to suprathermal electrons. For $v_{||} > 0$ and for relatively high values of v the function f_F can be represented analytically by a "bi-Maxwellian". Actually, the analytical form of the distribution that is used in the space physics literature^{19,23} to represent that observed for the superthermal electrons is isotropic and in addition has a discontinuity in its derivative in the region where it connects with the core distribution. That is, a distribution:

$$f_H = n_H / (2\pi T_H / m_e)^{3/2} \times \exp(-m_e v^2 / T_H)$$

is introduced with the requirement that :

$$f_H(v=v_B) = f_c(v=v_B) \text{ while } f_e = f_c \text{ for } v < v_B \text{ and } f_e = f_H \text{ for } v > v_B.$$

A survey of results obtained by various spacecraft indicate that :

$$0.02 \leq n_H/n_c \leq 0.05, 4 \leq T_H/T_c \leq 8 \text{ and } T_B = mv_B^2/2 \approx 7 T_c$$

In this connection, Olbert¹⁹ has suggested that there may be enough suprathermal electrons in the lower corona to provide an amount of heat flux sufficient to account for the entire energy flux observed in the far solar wind. In fact, Olbert and Scudder²⁴ have proposed that the suprathermal electron observed for $r > 0.3$ AU are direct remnants of the Maxwellian electron distribution that should exist in the lower solar corona. The rationale for this is that suprathermal electrons have very long collision mean-free paths and their distribution does not relax to that of the local Maxwellian as they travel away from the Sun along a given magnetic tube of force.

Recently the solar wind electron distribution has been reconstructed on the basis of experiments that allow for a better resolution in velocity space than those we have quoted so far. In particular, it appears that a distribution with a significant tail of the type assumed to explain the "slide away" regime²² observed in laboratory experiments, (see Fig. 10) be present²⁵.

While these observations and ideas have to undergo further analysis, it has become clear that the theoretical concept of a spherically symmetric, "thermally-driven wind",²⁶ can no longer go unquestioned. In this model, the driving heat flow is estimated on the basis of the "classical"² formulation of the electron thermal conductivity in the direction of the magnetic field that assumes the electron distribution to be very close to a Maxwellian, takes into

account only the effects of discrete collisions between particles, and does not include those of plasma collective modes such as microinstabilities² that have been shown frequently to be prevalent in laboratory experiments. In particular, the heat flow estimated on this basis, from the plasma temperatures and densities at the coronal base above the holes that are the sources of the solar wind observed further down-stream, falls short by an order of magnitude relative to that required by the appropriate energy balance¹⁹.

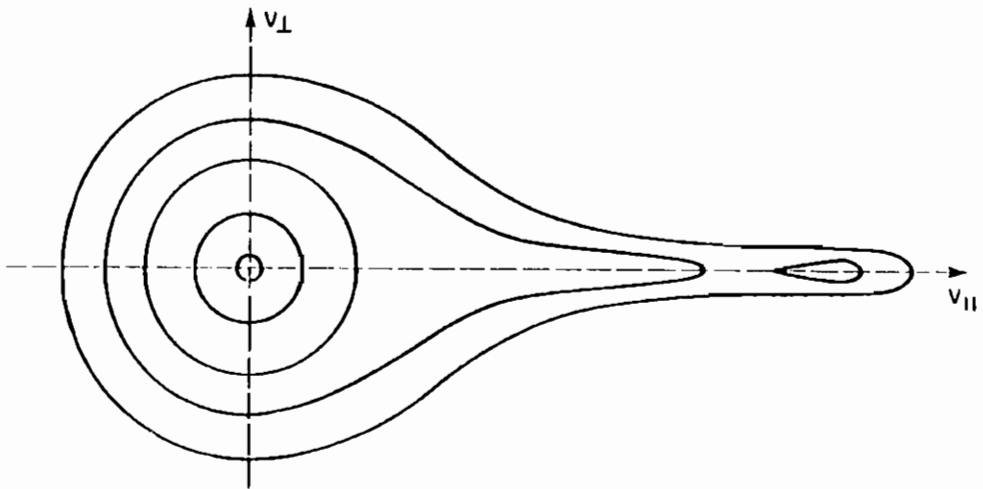


Figure 10: Example of a "slide-away" electron distribution²².

3. MAGNETIC FIELD CONFIGURATION

In addition to an evident radial structure, the solar wind has pronounced azimuthal features in all of its macroscopic parameters. For instance, in steady state conditions, regions where the "asymptotic" (that is evaluated at an approximate distance of 1 AU) wind speed falls into three intervals can be recognized;

- a) "high velocity streams" with speeds larger than 500 km/sec;
- b) "average wind" with speeds between 400 and 500 km/sec (most of the presently available data concern this regime);
- c) "slow wind" with speeds below 400 km/sec.

The azimuthal variability of the wind plasma parameters is usually observed as a function of time, in the spacecraft frame of reference, given the motion of the

spacecraft relative to that of the solar wind. Clearly, the exception to this is the occurrence of transient, intrinsically time dependent phenomena, which are quite common.

The existing analytical models of the heliospheric magnetic fields²⁷ assume a large-scale field line geometry conforming to the spiral pattern that is the result of a magnetic field originating on a rotating body and being "frozen in"² to a radially expanding plasma as we have indicated earlier. The so-called frozen-in-law is in fact expressed by the equation

$$(3) \quad \underline{\mathbf{E}} + \frac{1}{c} \underline{\mathbf{v}} \times \underline{\mathbf{B}} = 0$$

where $\underline{\mathbf{E}}$ is the electric field, $\underline{\mathbf{B}}$ the magnetic field, and $\underline{\mathbf{v}}$ the bulk (low) velocity. We refer to the spherical coordinates r , θ and ϕ where r is the heliocentric distance, θ the heliographic latitude and ϕ the longitude (azimuth). We consider the velocity $\underline{\mathbf{v}}_0 = \omega_0 r \cos\theta \underline{\mathbf{e}}_\phi$ of co-rotation with the Sun and assume that over a certain portion of the Sun surface \mathbf{B} is radial and parallel to

$$(4) \quad \underline{\mathbf{v}}' = \underline{\mathbf{v}} - \underline{\mathbf{v}}_0$$

Here ω_0 is the frequency of rotation of the Sun ($\omega_0 \approx 2.9 \times 10^{-6} \text{sec}^{-1}$). Then we can argue that, in a stationary state

$$(5) \quad \underline{\mathbf{v}} \times \underline{\mathbf{B}} = 0$$

everywhere and no electric field is seen in the co-rotating frame. Consequently, the magnetic field lines coincide with the plasma stream lines as seen from the co-rotating frame of reference.

The conservation of mass and magnetic flux implies

$$(6) \quad \underline{\mathbf{B}} = c n \underline{\mathbf{v}}$$

where c is constant along a given magnetic field line. In particular we have

$$(7) \quad \frac{nv_r}{B_r} = c$$

where

$$(8) \quad B_r \propto \frac{1}{r^2} .$$

If we also assume that $v_\phi \ll v_0$ we have

$$(9) \quad \frac{B_\phi}{B_r} = \frac{\omega_0 r \cos \theta}{v_r}$$

and this implies that:

- a) the magnetic field lines lie on cones with $\theta = \text{constant}$
- b) the magnetic field \underline{B} forms an angle χ with the radial direction (the so-called "garden hose angle") given by

$$(10) \quad \text{tg } \chi = \frac{r \omega_0}{v_r}$$

If we take v_r to be approximately the observed wind velocity, at the orbit of the Earth where $v \approx 3.6 \times 10^7$ cm/sec we obtain $\chi \approx 50^\circ$.

If this picture is correct the field should become more radial at high latitudes where the plasma flow is faster and the rotational effects are weaker. The interplanetary magnetic field components¹⁹ are represented in Fig. 11,

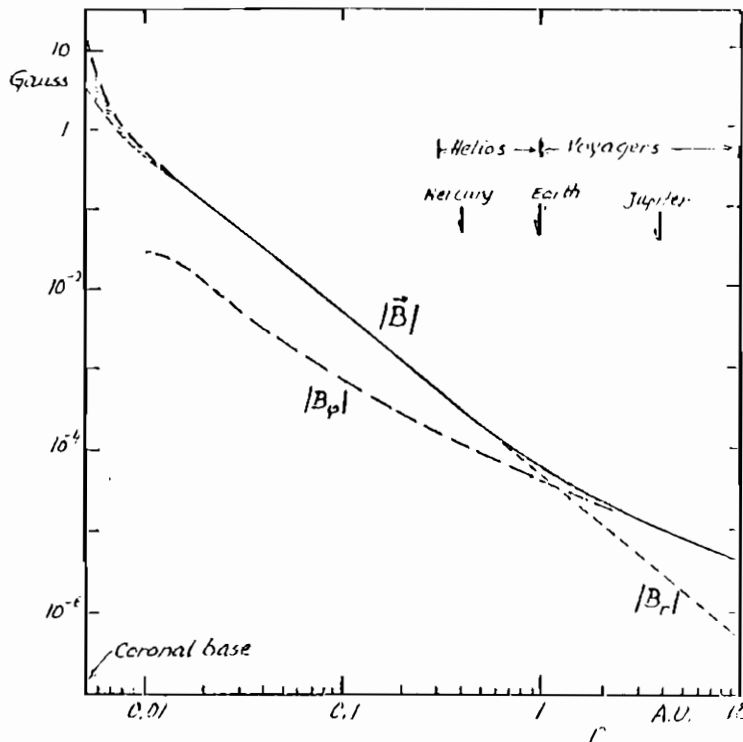


Figure 11: Components of the interplanetary magnetic field as a function of the heliocentric distance¹⁹.

where the magnitude of the magnetic field $|\underline{B}|$ is normalized to 5γ at 1 AU ($1\gamma = 10$ microgauss). For $r > 2r_{\odot}$ ($r_{\odot} =$ radius of the Sun) the given curves have been derived analytically from the just mentioned "spiral model", but they are consistent with all spacecraft observations for a quiet Sun. This consistency exists only for the average field and not for the finite amplitude fluctuations that often conceal the average profile. It is also well established that the spiral model does not hold in the region $r_{\odot} < r < 2r_{\odot}$. There the field contains also a strong B_{θ} component besides the B_r and B_{ϕ} components. In particular the field profiles that appear to be appropriate over coronal holes have a much steeper descent than $1/r^2$. Notice that the considered interval for the variable r goes from the base of the corona at $r = 5 \times 10^{-3}$ AU to Saturn at 10 AU.

An important feature of the interplanetary field observed on the ecliptic plane is the magnetic polarity sector structures. The field that sweeps past near-Earth satellites is characterized by two or four, and occasionally even six, regions having alternately positive (outgoing) and negative (ingoing) polarity per rotation. This pattern has been observed to persist over many solar rotations²⁸. The intervals of similarly directed field lines have been termed sectors. The transition from one sector to the next, the sector boundary, often precedes the arrival of a fast stream. The sector boundaries correspond to a large scale neutral sheet (Fig. 12) that is co-rotating with the Sun and

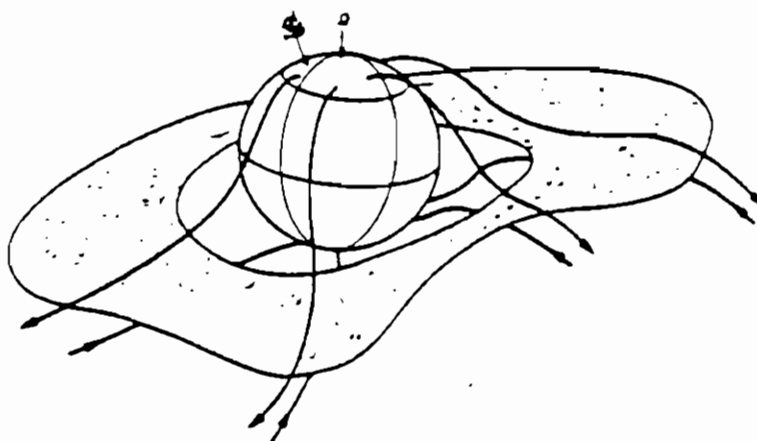


Figure 12: Sketch of the current sheet that is thought to be responsible for the sector structure. The axis of the current sheet, M , is considered to be tilted with respect to the solar rotation axis, Ω^{10} .

separates the inward and outward components of a field configuration

originating from a dipole-like solar field. In-ecliptic observations indicate that this neutral sheet is inclined about 12° relative to the solar equator. The simplest neutral sheet configuration in which the magnetic field vanishes is represented in Fig. 13 together with the relevant current density distribution.

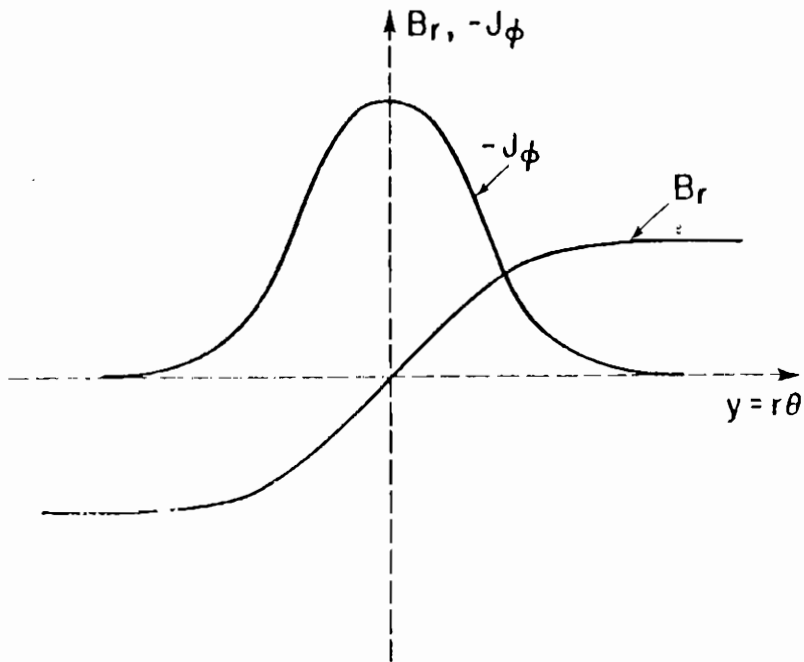


Figure 13: Magnetic field and plasma current density distribution in a neutral sheet.

At the Earth one dominant magnetic field polarity or the other is seen depending on whether the observer is above or below the current sheet. It also appears that the current sheet is inclined with respect to the solar equator, so that at the Earth two sectors should be seen as the Sun rotates. Four or six sectors can appear when the current sheet itself develops large-scale warps or undulations. The warps in the current sheet appear to be caused by the fast streams, which carry out fields from coronal holes located closer to the equator at more central parts of the Sun disk²⁹. We notice that a magnetic field configuration with a neutral sheet, where the field vanishes, exists in the Earth magnetotail and it is possible that several of the physical processes that have been studied for the Earth's neutral sheet³⁰ will be of interest for the solar wind current sheet. Among these we may mention those involving magnetic reconnection², that is a breakdown of the frozen-in-law introduced earlier.

Propagation of energetic solar particles (see Section 5) in the interplanetary medium is affected to a large degree by the existence of so-called Co-rotating Interaction Regions (CIRs) (see Ref.[31]). These have been observed as recurring regions of enhanced magnetic field magnitude³² sharply bounded by jumps in solar wind velocity that begin to develop beyond 1.5 AU, and frequently accompanied by shocks at the boundaries beyond ~2.5 AU. These structures result from high-velocity solar wind streams overtaking lower-velocity streams. If the source of the streams are time stationary, and associated with different coronal holes, these regions appear as discrete, large interplanetary structures co-rotating with the Sun as illustrated in Fig. 14. The zone between successive CIRs is considered to

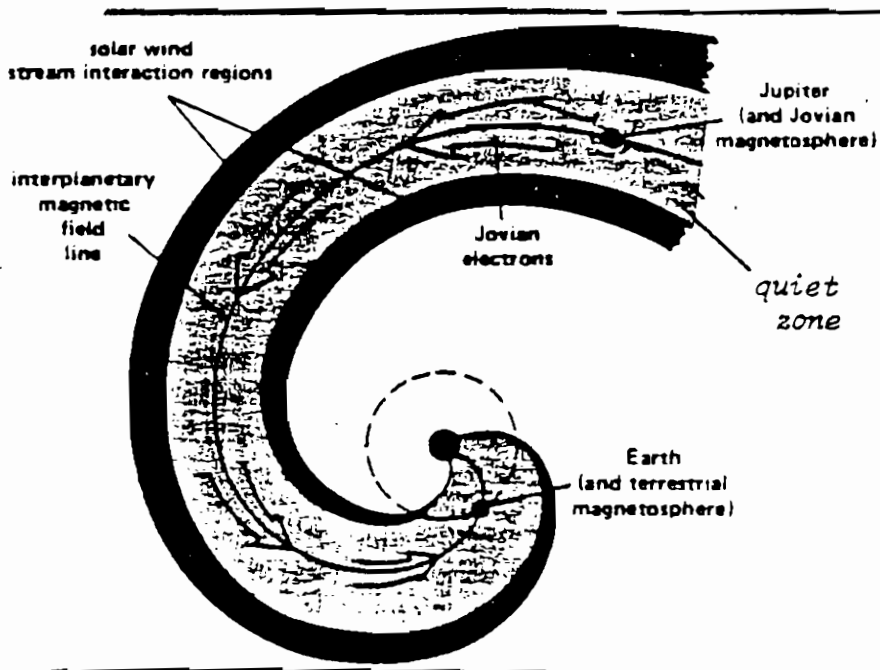


Figure14: Co-rotating Interplanetary Region (CIR). The dark spiraling curves illustrate two stream regions, such as result from solar wind emitted by coronal holes. The cavity between them can form a conduit for electrons from the Sun and possibly from Jupiter, which travel along interplanetary magnetic field lines to Earth, where they appear to affect the magnetosphere³¹.

have a stochastic field distribution and have been observed to provide a "channel" of communication between the magnetospheres are particles that

were originally accelerated in Jupiter's magnetosphere³¹. Jupiter and Earth align themselves in the same position relative to the Sun every 13 months. When proper alignment occurs, the fluxes of high-energy electrons within our magnetosphere increase. In other words, electrons accelerated in Jupiter's magnetosphere, escape from the Jovian system, move along the zone between successive CIRs, and reach the Earth's magnetic field.

Interplanetary scintillation observations, utilizing the scattering of electromagnetic radiation from radio sources, indicate that the solar wind bulk velocity increase with increasing latitude away from the ecliptic when averaged on a global scale³³. The fast, high-latitude wind is generally accepted as originating in the large-scale polar coronal holes, and it is expected that stream interaction will be largely absent in these high latitude regions. If this expectation is correct, spacecraft exploring high latitude regions should observe a "quiet" solar wind, in contrast with the solar wind available to in-ecliptic that is characterized by interactions between streams of different velocities, as we have indicated. We also notice that measurements of the interplanetary magnetic field over the polar regions could allow an extrapolation to the solar photospheric field, without the complex field tracing necessary at low latitude. Knowledge of the polar surface field is important in relation to theories of solar dynamo¹¹.

4. MACROSCOPIC PLASMA PARAMETERS

The radial dependence of macroscopic wind parameters such as the particle density, the flow velocity, and the "temperature" can only be inferred from a combination of several direct and indirect measurements and of rather questionable theoretical assumptions. In particular, as we have indicated earlier, the measured particle distributions in velocity space cannot be characterized always by a single temperature. In fact, Fig.15, which gives the electron density profile¹⁰ has been obtained from direct density measurements for $r > 0.3$ AU taken by the Helios and Voyager spacecrafts and the indirect measurements, obtained from coronal electron scattered light, zodiacal light, dispersion of signals from pulsars, etc. The curve indicated by the solid line can be constructed only after assuming a steady state spherical solar wind model with an asymptotic bulk velocity of 400 km/s and has to be viewed as a kind of "average". Notice that the density profiles for the region above the polar coronal hole and for the high velocity streams lie below the "average", while that for the slow wind lies above.

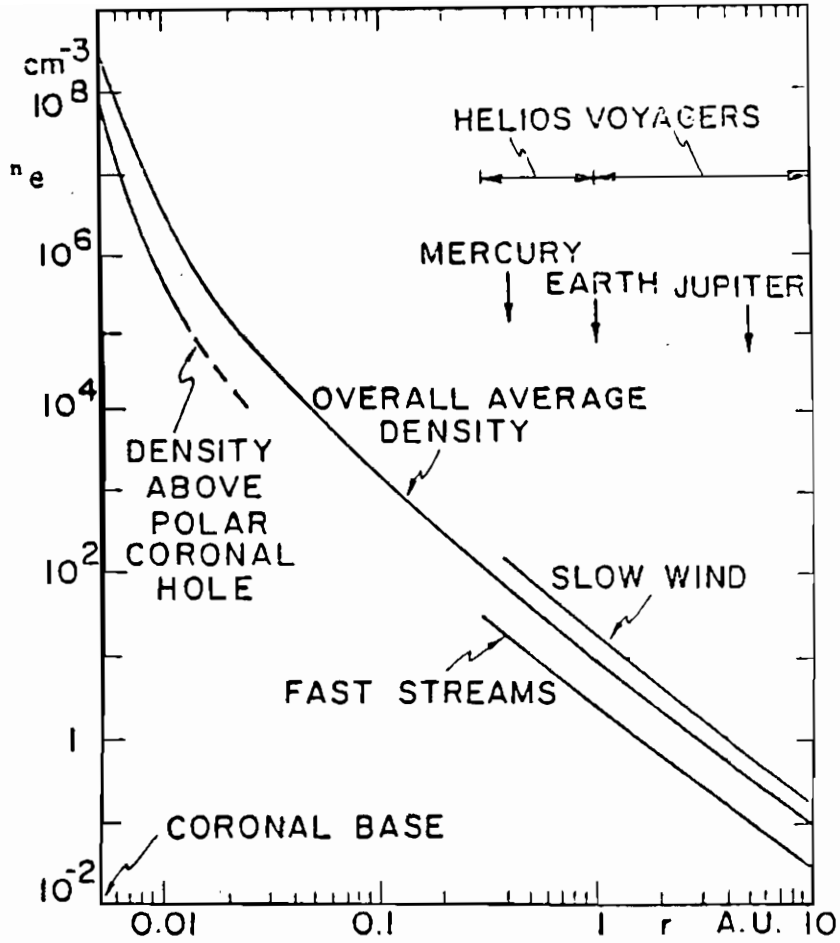


Figure 15: Dependence of the plasma density on the heliocentric distance¹⁹.

Figure 16 has been evaluated from the profiles of Figs.11 and 15 for the "average wind" ($n=7 \text{ cm}^{-3}$ and $v=400 \text{ km/s}$ at 1 AU). The radial component of the wind velocity V_r has been obtained from the expression

$$(7') \quad \frac{v_r(r) n(r)}{B_r(r)} = \left(\frac{n v_r}{B_r} \right)_{r=1\text{AU}}$$

that is a consequence of the "spiral model" [see Eq.(1)]. The Alfvén velocity $v_A \equiv B / (4\pi n m_p)^{1/2}$, m_p being the proton mass serves as a reference to indicate that when $v_r > v_A$, at $r \geq 20 r_\odot$, the observation of magnetohydrodynamic shock waves can be expected¹⁹. In fact v_A is the characteristic velocity of magnetohydrodynamic waves in a magnetized plasma².

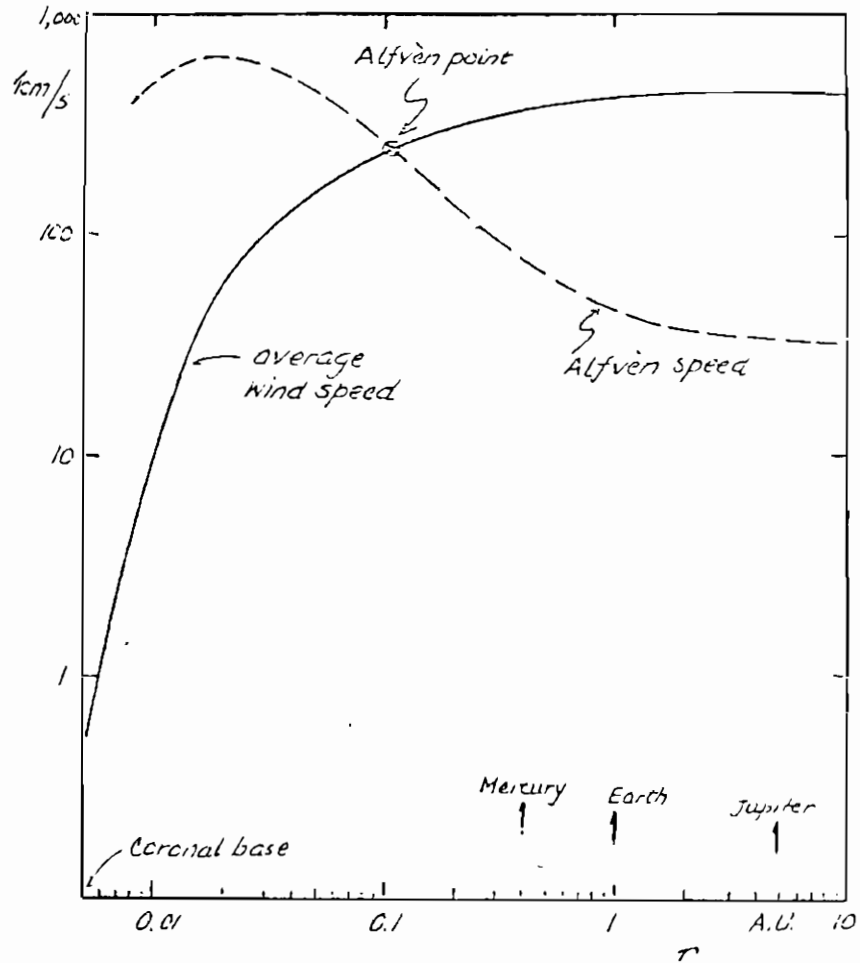


Figure 16: Radial component on the wind velocity and alven ware velocity¹⁹.

Clearly, the term "the asymptotic wind velocity", has been used in the context of Fig. 17.

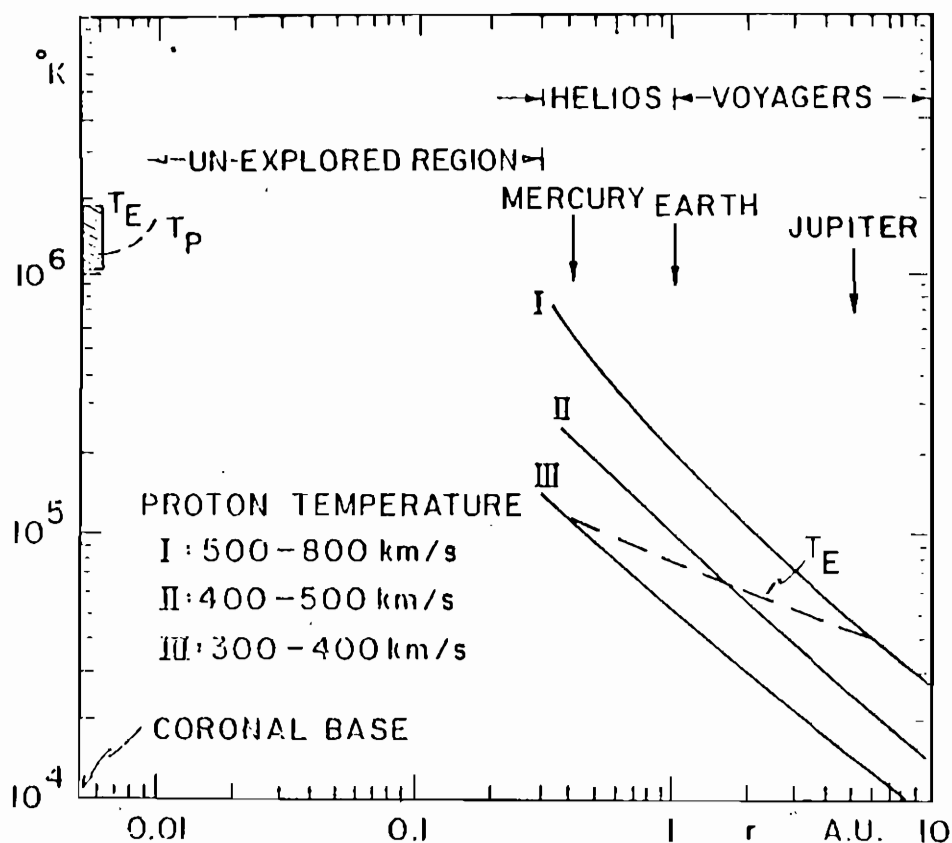


Figure 17: Proton and electron temperature trends as a function of the heliocentric distance¹⁹.

Some of the trends of the plasma temperature, to the extent that it is possible to speak of one, are represented in Fig. 17. We note that the information relevant to the region $r < 0.3$ AU is either very poor or nonexistent. Assuming the proton distribution function in velocity space to be represented by a low-temperature Maxwellian, the indicated temperature is

$$T_P = \frac{2}{3} T_{\perp} + \frac{1}{3} T_{\parallel}$$

and the labels I,II,III refer to the three groups of wind defined earlier in this section. In particular, we see that the ion temperature increases with increasing wind velocity. The high velocity streams achieve transverse temperatures as high as 10^6 degrees at ≈ 0.3 AU.

The electron distribution can be seen roughly as the superposition of two Maxwellians, characterized by the temperatures T_c and T_H as indicated in Section 3. The dashed lines in Fig. 17 represent the profiles of T_c .

Finally we note that in addition to the azimuthal structure of the solar wind it is important to consider that there are intrinsically time-dependent phenomena, as indicated for instance in Fig. 18. Here we can see three wind velocity discontinuities indicating the passage of three shocks. It is not common to find three shocks during one solar rotation but, at distances beyond Mars, the frequency of shock occurrence does grow with distance; one shock per solar rotation is a typical average.

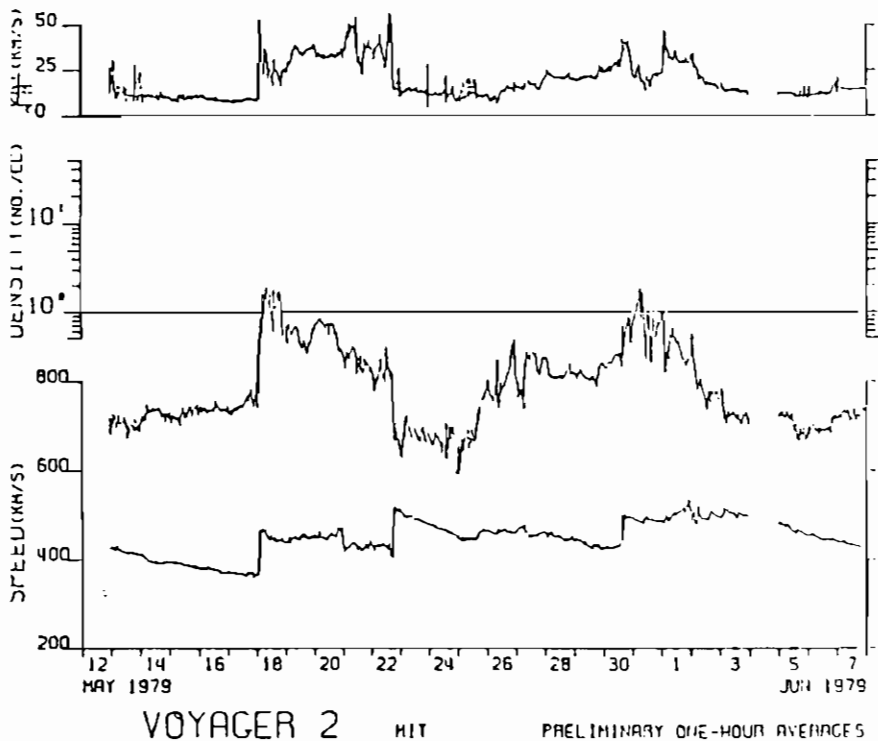


Figure 18: Proton thermal velocity, plasma density and wind velocity monitored by the Voyager II spacecraft during one solar rotation when the spacecraft was near 10 AU¹⁹.

5. "OTHER" COMPONENTS AND EFFECTS OF FLARES

As indicated earlier, cosmic ray particles arriving at the inner heliosphere from interstellar space represent, together with interstellar dust and neutral gas, the only available sample of matter originating outside the solar system.

In the case of cosmic rays, in order to extract the maximum amount of information contained in their composition and energy spectra and concerning their source and histories, it is essential that the relevant "modulation" introduced by the heliospheric plasma environment be adequately understood¹¹. Given the predicted, near-radial magnetic field configuration at high latitudes, it is possible that the spectrum of galactic cosmic rays will not be significantly affected when they enter the heliosphere over the poles. On the other hand, recent models suggest (see Ref. [34]) that particle drifts due to the heliospheric magnetic field may seriously limit access over the poles, an effect that depends on the dominant polarity of the local magnetic field.

The existence of a neutral particle component in the heliosphere was first considered in order to explain the observed extraterrestrial origin of the diffuse optical radiation with wavelength of $121.6 \times 10^{-3} \mu\text{m}$ (so-called Lyman- α). It has since been shown (Ref.[35]) that, owing to the motion of the solar system through the local interstellar medium, neutral interstellar hydrogen and helium atoms can penetrate into the heliosphere with a velocity of about 20 km s^{-1} , and resonantly scatter the solar radiation at wavelengths of $121.6 \times 10^{-3} \mu\text{m}$ and $58.6 \times 10^{-3} \mu\text{m}$.

Despite the important role played by the interstellar gas in determining, for example, the position of the terminating boundary of the heliosphere, very little is known about the important parameters of the gas in the vicinity of the solar system. Current knowledge is indirect, based only on measurements of the resonance radiations discussed above; no direct, in situ observations of the neutral atoms have yet been made.

Another important component of the heliosphere is the interplanetary dust. Although the total mass of the interplanetary dust is negligible compared to larger solar system bodies, identification of the sources and of the processes which limit 10^5 years (Ref.[36]) is of relevance to our understanding of the role played by dust in astrophysical system.

Finally we noted that an important class of the high (relativistic) energy charged particles that are found in the heliosphere is that produced by solar flares. The processes which result in the particle behaviour observed near the Earth, that is acceleration, coronal propagation, and interplanetary propagation, have yet to be adequately identified. It is expected that the extent to which each of these processes contributes to the characteristics of

the "quiet" solar wind will vary with heliographic latitude due to the changing conditions in the corona. The importance of understanding coronal propagation is emphasized by the fact that solar particles have been observed in the ecliptic to be released as far as 180° in heliographic longitude from the site of an optically observed flare³⁷. Relative chemical and isotopic abundances, on the other hand, are more likely to be characteristic of the solar flare acceleration process itself when measured at middle latitudes corresponding to the active regions on the Sun, as they should not be altered drastically by propagation effects. We also notice that the presence of interplanetary shock waves, can play an equally important role in propagating, and possibly accelerating, energetic charged particles.

Solar flares have been observed to induce streams. In particular, a flare can initiate a large, explosive release of coronal material which arrives at the Earth after two to three days in the form of a shock front that has swept up the plasma and magnetic field ahead of it. The highest flow speed is observed to follow the shock, and behind the shock a characteristic shell of anomalously high abundance of α -particles is usually detected²⁹.

6. FINAL REMARKS

As was pointed out in the text, our knowledge of the heliosphere is very rudimentary and evolving rapidly as in situ measurements are being planned, carried out, and gradually analyzed. A considerable portion of the information we have presented is still rather morphological and qualitative, but it is in the character of science to comfort us with situations where what we begin to see and contemplate is far more than what we can describe and reduce into elegant mathematical formulations. It is also evident that this article has left aside the fascinating phenomena resulting from the interaction of the solar wind with the planet magnetospheres that have been explored so far (see for instance, Ref.[38]). In fact we feel that this topic deserves a separate treatment of its own after the data that have become available from recent space mission will have had the benefit of more theoretical elaboration.

It is a pleasure to thank J.Belcher and S.Olbert for their generous help, G.Bertin and F.Pegoraro for their timely and valuable comments, and G.Bernardini and L.Radicati for winning over my reluctance to write.

REFERENCES

- [1] A. Bonetti, H.S. Bridge, A.J. Lazarus, B.B. Rosi, and F. Scherb, in Pontificiae Academiae Scientiarum Scripta Varia, 25, (1963); and J. Geophys. Res. 68, 4017 (1963).
- [2] B. Coppi, Massachusetts Institute of Technology, R.L.E., Report PRR-72-1 (Cambridge, MA, 1972). Updated and translated version in Enciclopedia del Novecento, Eds. G. Bernardini and L. Radicati. Istituto della Enciclopedia Italiana (Rome, 1981), Vol. V, p. 380.
- [3] H.S. Bridge, et al., Science 204, 987 (1979).
- [4] J.W. Belcher, et al., in Solar Wind 4, Ed. H. Rosenbauer. Springer Verlag (1979).
- [5] W.I. Axford, Space Science Rev. 14, 582 (1973).
- [6] T.E. Holtzer, in Solar System Plasma Physics, Eds. C. Kennel, L. Lanzarotti and E. Parker. North-Holland (New York, 1979), p. 145.
- [7] E.N. Parker, in Frontiers in Astronomy, Ed. O. Gingerich, W.H. Freeman & Co. (San Francisco, 1970) p. 98.
- [8] L. Biermann, Z. Astrophys. 29, 274 (1951).
- [9] E.N. Parker, Astrophys. J. 128, 664 (1958).
- [10] E.J. Smith, B.T. Tsurutani, R.L. Rosenberg, J. Geophys. Res. 83, 717 (1978).
- [11] R.G. Marsden, and K.-P. Wentzel, in Plasma Astrophysics, Eds. T. Guyenne and G. Levy. European Space Agency (Paris, 1981), p. 167.
- [12] S.I. Akasofu, and S. Chapman, Solar-Terrestrial Physics. Oxford Univ. Press, Oxford, England, (1972).
- [13] L.F. Burlaga, and K.W. Ogilvie, J. Geophys. Res. 78, 2028 (1973); L.F. Burlaga, Space Sci. Rev. 17, 327 (1975).
- [14] J.W. Harvey, and M.R. Sheeley, Space Sci. Rev. 23, 139 (1979).
- [15] A.S. Krieger, et al., Astrophys. J. Letters L47, 185 (1973).
- [16] R. Rosner, L. Golub, B. Coppi, G.S. Vaiana, Astrophys. Journal 222, 317 (1978).
- [17] A.J. Hundhausen, in Coronal Holes and High Wind Streams, Ed. J.B. Zirker. Colorado Ass. Univ. Press, (Boulder, 1977) p. 225.
- [18] R.H. Levine, M.D. Altschuler, J.W. Harvey, J. Geophys. Res. 82, 1061 (1977).
- [19] S. Olbert, in Plasma Astrophysics, Eds. T. Guyenne and G. Levy. European Space Agency (Paris, 1981) p. 135.
- [20] E. Marsch, et al., J. Geophys. Res. 87, 35 (1982), and J. Geophys. Res. 87, 52 (1982).

- [21] C.C. Goodrich, Private Communication (1981).
- [22] B. Coppi, F. Pegoraro, R. Pozzoli, and G. Rewoldt, Nucl. Fus. 16, 309 (1976).
- [23] W.C. Feldman, et al., J.Geophys. Res. 80, 31, 4181 (1975).
- [24] J.D. Scudder and S. Olbert, J.Geophys. Res. 84, 2755 (1979); J. Geophys. Res. 84, 6603 (1979).
- [25] S. Olbert, Private Communication (1982).
- [26] E.N. Parker, Interplanetary Dynamical Processes. Interscience, (New York, 1963).
- [27] R.L. Carovillano, and G.L. Siscoe, Solar Phys. 8, 401 (1969).
- [28] J.M. Wilcox, and N.F. Ness, J. Geophys. Res. 70, 5793 (1965).
- [29] J.V. Evans, Science 216, 467 (1982).
- [30] B. Coppi, G. Laval, and R. Pellat, Phys. Rev. Letters 16, 1207 (1966).
- [31] T.F.Conlon, and J.A. Simpson, Astrophysics J. 211, L45 (1977).
- [32] E.J. Smith, and J.H. Wolfe, Geophys. Res. Lett. 3, 137 (1976).
- [33] W.A. Coles, Nature 286, 239 (1980).
- [34] J.R. Jokipii, and D.A. Kopriva, Astrophys. J. 234, 384 (1979).
- [35] P.W. Blum, and H.J. Fahr, Astron & Astrophys. 4, 280 (1970).
- [36] F.L. Whipple, NASA Document SP-150, 409 (1967).
- [37] R.B. McKibben, J. Geophys. Res. 77, 3957-3984 (1972).
- [38] J.W. Belcher, in Plasma Astrophysics, Eds. T. Guyenne and G. Levy. European Space Agency (Paris, 1981) p. 129.

Bruno Coppi

Massachusetts Institute of Technology

Francesco Pegoraro

Scuola Normale Superiore

THE IGNITOR PROJECT

The Ignitor concept was the first experiment (see Fig.1) proposed and designed in order to achieve, on the basis of existing technology, the conditions where a deuterium-tritium plasma can ignite¹).

Ignition occurs when the energy deposited by the charged fusion reaction products in the plasma compensates all forms of energy losses. These include radiation emission and particles and energy transport, resulting mostly from the excitation of plasma resistive modes and only in part from the effect of interparticle collision. Thus a fusion burning plasma that contains a nearly monochromatic source of multi-Mev particles is inherently a system that departs drastically from thermal equilibrium. The limited validity of the theoretical description that have been formulated for this kind of systems makes it particularly important to have experiments readily available to gather key information on the nature of the collective modes (e.g. various forms of instability and plasma turbulence) that characterize an ignited plasma.

Since the Ignitor concept was introduced in 1975 and later developed, other advance experimental facilities (in particular TFTR in the US and JET in Europe) have been redesigned and allowed to extend their performances in order to come as close as possible to some design characteristics embodied in Ignitor. In the case of TFTR the magnetic field was raised and in the case of JET the maximum plasma current and the magnetic field associated with it were increased well above the reference values of their original design, while a phase of tritium operation was included in both programs.

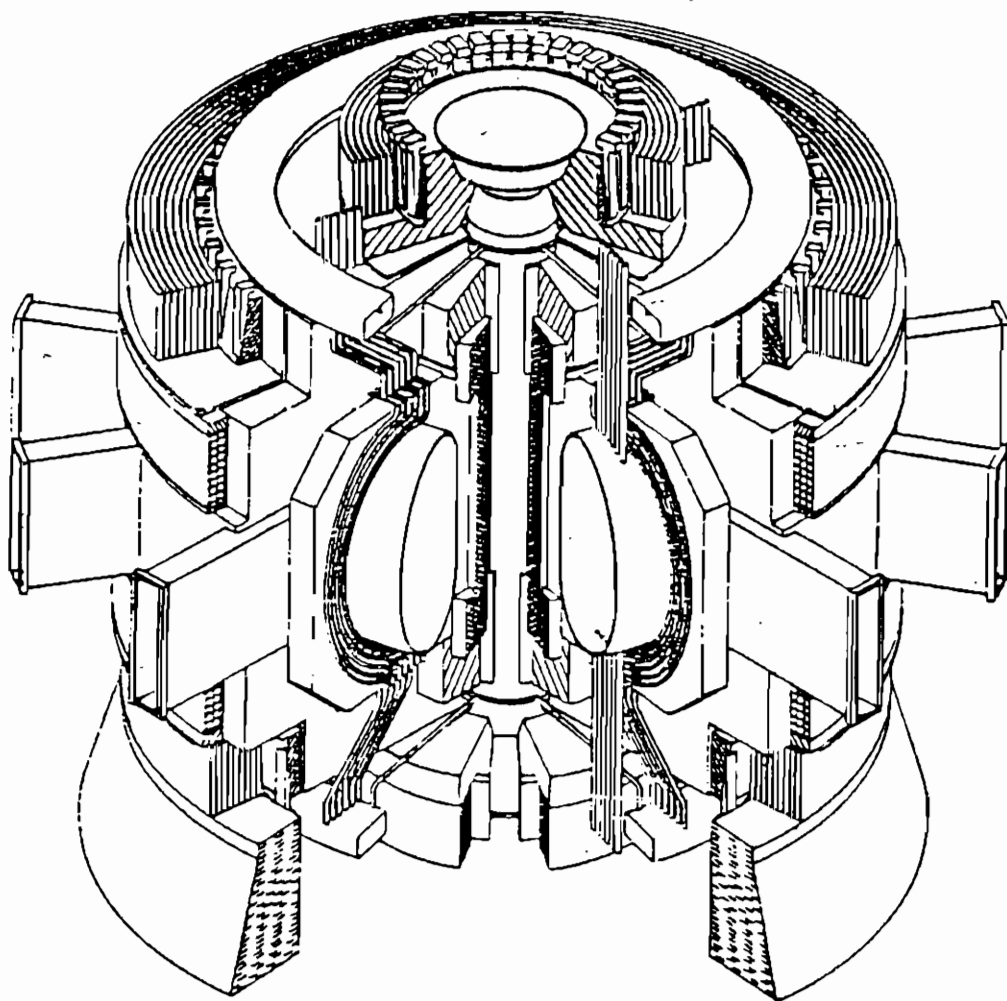


Figure 1: View of the Ignitor experiment

By now, one of the criteria that is commonly accepted as rating the potential performance of a toroidal machine as a confiner of the burning plasma is the value of the "strengh parameter":

$$F_s = I_p B_p$$

where I_p is the plasma current and B_p is the value of the magnetic field associated with it. On the basis of this, a comparison of Ignitor with existing advanced experimental devices is shown in Fig.2.

Another point to underline is that the containment of the charged fusion reactions products, on the basis of single particle orbit considerations, requires in practice a minimum plasma current of about 3 megampere in the case of the 3.5 MeV α -particles and about 6 megampere in the case of the 14.7 MeV protons produced by the D-He³ reactions. The maximum current considered in the present Ignitor design is about 11 megampere and is therefore sufficient to begin the study of the effect of D-He³ reactions. However on the basis of present day knowledge, the other device characteristics are not adequate to reach conditions where substantial heating from D-He³ reactions can be produced. To attain such conditions an extension of the Ignitor line has been envisaged, following the proof obtained at the beginning of the 80's that, contrary the previous expectations, advanced fuel (D-D, D-He³) reactors are feasible²⁾ on the basis of our theoretical understanding. In this ontext we recall that the development of D-He³ reactors is of great practical relevance, as in a D-T reactor most of the enrgy is released in the form of energetic neutrons. The activation and the damage caused by the neutrons to the materials surrounding the plasma chamber are avoided in a D-He³ reactor where the fuel is non radioactive and the reaction products consist almost exclusively of charged particles that can be guided by electromagnetic fields. However, similarly to Tritium that has a lifetime of approximately 12 years and decays into He³, He³ is extremely scarce on Earth and must be produced. Present reserves of He³ are sufficinet for an experimental program, given in particular the large number of warheads that have been stockpiled. For an application on a wider scale, the possibility has been studied of building deuterium-deuterium reactors in isolated locations, far from populated areas, and of devoting them to the production of He³ reactor, but releases about 40% of its energy in the form of neutrons.

The guiding criterion in choosing the parameters of Ignitor is to advance the onset of effective α -particle heating to the lowest possible temperature. In particular the particle density of operation is maximized while taking into account all the constraints imposed by the temperature and the confinement time that havce to be achieved. In order to obtain the desirable density range,

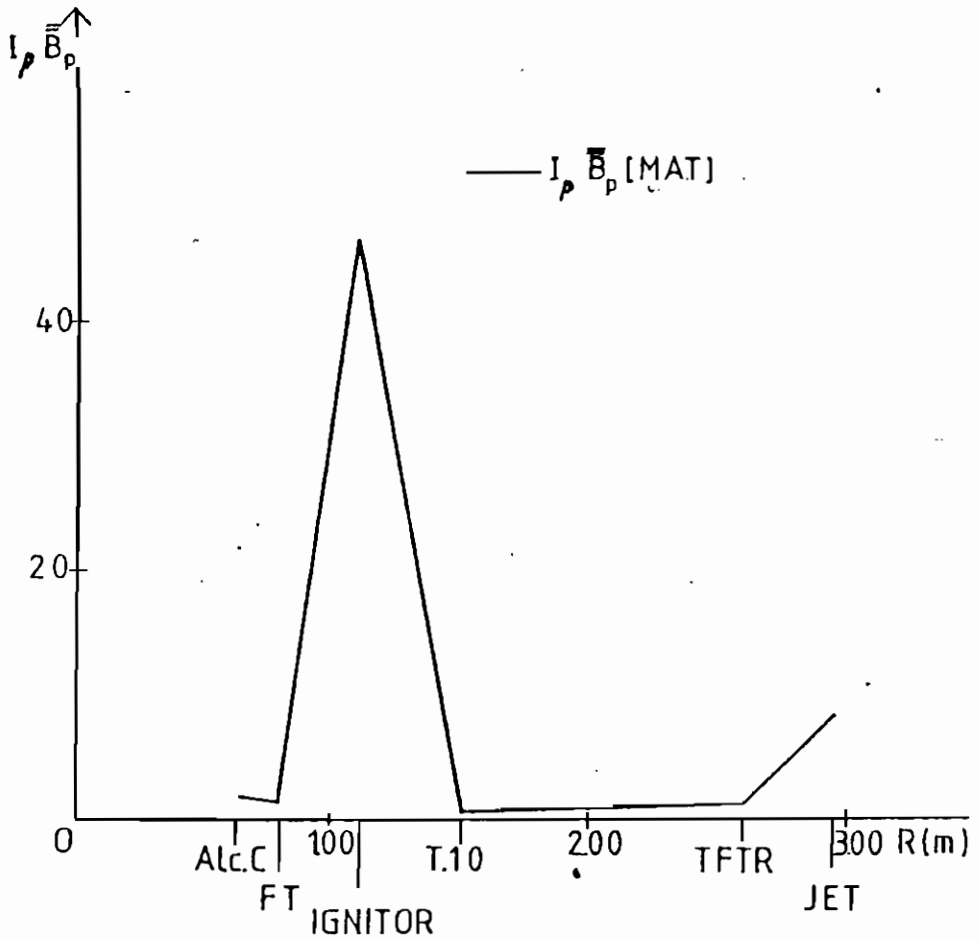


Figure 2: Rating of Ignitor versus existing advance confinement experiment in terms of the strength parameter $F_s = I_p \bar{B}_p$.

corresponding to a peak density $n_0 = 10^{15} \text{ cm}^{-3}$, the prescription that is adopted is the same for Alcator, i.e. to produce the highest possible average current density $\langle j_{\parallel} \rangle$ without exciting macroscopic instabilities. This guideline has been supported by an increasingly large body of experimental evidence. The average current density is:

$$\langle j_{\parallel} \rangle = (1.6 B_T R_0 q_E)$$

where B_T is the toroidal field, R_0 is the major radius and q_E is a "technical safety factor" that, for the toroidal configuration with low aspect ratio and non circular cross section considered, can be as low as 1.6 (see table 1). This explains why we consider experiments with high magnetic field and compact size.

We also notice that recent series of experiments performed on the TFTR machine³⁾ have confirmed the existence of well confined plasma states with reduced plasma currents as found in 1974 in the Alcator experimental machine. Thus we can expect that it will be possible to decrease the plasma current in the regime where the α -particle heating is prevalent without spoiling confinement. We recall that in 1974 an important discovery was made on the Alcator A device where it was found that the energy confinement time τ_E increases linearly with the plasma density, thus indicating a favourable n^2 dependence of the Lawson parameter $n\tau_E$ (see Fig.3). Indeed this positive result obtained in a compact device was instrumental in making it thinkable, as early as eleven years ago, that an experiment could be built with the genuine expectation of being able to reach ignition. A group of Italian scientists working at MIT had a central role in this discovery⁴⁾. This close collaboration continued and expanded, including several Italian Universities, research laboratories and Firms, in the years during which the Ignitor project was developed and led to the strengthening of a network of intellectual and scientific interest and expertise, that can provide an important guarantee for the successful realization of the project.

In assessing the degree of advancement of existing confinement experiments, relative to the conditions needed for ignitor, it is necessary to weigh a variety of factors such as the degree of the plasma purity and the value of the electron temperature, and the conditions under which these are obtained. Instead, a common, often misleading, practice is to assign each experiment a point in the familiar $(n\tau_E, T)$ plane using for instance the electron density, the ion temperature or the electron temperature without specifying whether Z_{eff} , the effective charge number, is close to unity. In fact, the relevant quantity to consider is the peak deuteron density, as this is representative of the plasma reactivity, that, when $Z_{\text{eff}} > 1$, can be considerably smaller than the peak electron density n_{e0} . Moreover, in an

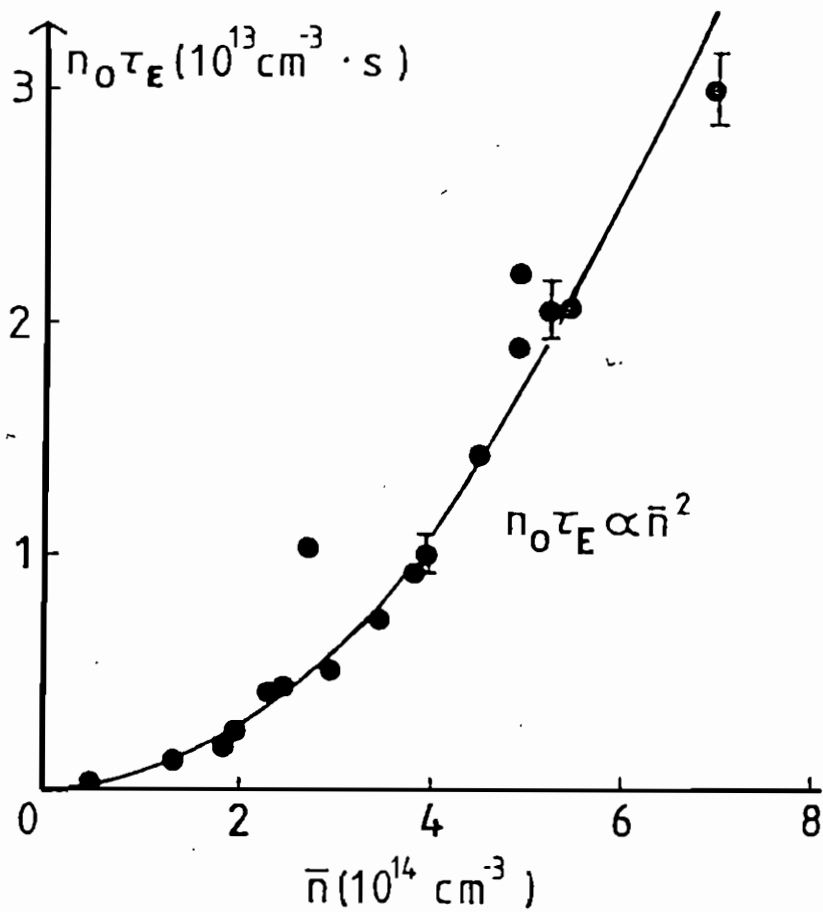


Figure 3: The discovery of the so called 'Alcator Scaling' for the confinement parameter $n_0 \tau_E$.

igniting plasma the peak electron temperature T_{eo} exceeds T_{io} , the peak ion temperature, as most of the α -particle energy is deposited on the electron population and then transferred to the reacting nuclei. In addition, it is important that Z_{eff} be quite close to unity, as this affects the ignition conditions seriously. On the other hand, both T_{eo} and the energy replacement time τ_E have been observed to increase with Z_{eff} in most experiments. Therefore, we argue that n_{D0} , T_{eo} ($Z_{eff}=1$) and τ_E ($Z_{eff}=1$) should be used in the appropriate $(n\tau_E, T)$ diagram instead of n_{eo} , T_{io} and τ_E ($Z_{eff} > 1$). Alternatively, the experimentally obtained values of n_{D0} , τ_E ($Z_{eff} > 1$) and T_{eo} ($Z_{eff} > 1$) should be related to the ignition curve $(n\tau_E, T)$ that would be obtained for the same values of Z_{eff} .

In addition to this, in order to assess the degree of advancement of a given experiment fairly, it is important to take into account the fact that when its linear dimensions are reduced, all the intrinsic time scales become shorter.

In particular, we observe that the type of plasma collective modes influencing the effective energy transport have their frequencies and growth rates related to the average electron transit frequency:

$$\omega_{te} = v_{the} \frac{2\pi}{L}$$

where L is the periodicity length of the magnetic field lines ($L = 2\pi q R$ for an axisymmetric toroidal configuration). This frequency expresses the obvious fact that all relevant physical processes are faster in smaller experiments. Consequently, on the basis of the previous considerations we propose, as an intrinsic parameter of merit, the effective pressure:

$$P_{eff} = n_{D0} T_{eo} \tau_E \omega_{te} ,$$

and we refer, in addition to the $n_{D0}\tau_E$ versus T_{eo} plane, to the plane P_{eff} versus the length of the plasma column. If we follow these criteria the compact line of experiments that is represented by the Alcator machines of MIT and includes the FT device of the Frascati Laboratories still occupies the top position. This becomes even more striking if, instead of P_{eff} , we take a parameter of merit that includes instead of τ_E , the associated diffusion coefficient:

$$\bar{D}_E \equiv \frac{4\bar{a}^2}{\tau_E (Z_{eff} = 1)}$$

and we introduce the intrinsic parameter of advancement:

$$A = \frac{n_{oD} T_{eo} (Z_{eff} = 1)}{D_E}$$

The Ignitor design, as indicated earlier, tends to maximize the role of ohmic heating, up to the point where this is not overwhelmed by α -particle heating. We can expect the confinement time τ_E to follow the scaling laws that we have learned from present day experiments. In this case we find that the extrapolated confinement parameter $n_o \tau_E$ considerably exceeds the value needed to achieve ignition.

We refer, in particular, to the recently reported results of the experiments⁵⁾ that were carried out on the Asdex machine where the plasma cross section is about $40 \times 40 \text{ cm}^2$. The energy replacement time, corresponding to a line average density $\langle n \rangle$ of about 10^{14} cm^{-3} , is about 160 msec. Consequently, if we assume for simplicity that τ_E scale as $\langle n \rangle^{-1/2}$, where $a = \sqrt{ab}$, and that the appropriate density of operation of Ignitor corresponds to about $n \cong 5 \times 10^{14} \text{ cm}^{-3}$, the value of τ_E would be approximately 1.5 sec. This is higher by about a factor 4 than what is needed for ignition and represents therefore a considerable safety margin for Ignitor.

A significant safety margin can be argued to exist also in obtaining plasmas with Z_{eff} close to unity as this parameter has been observed to approach unity in all experiments when the density is increased toward the values we have just mentioned.

We may also consider a series of design parameters of merit⁶⁾ in order to rate the ability of a given experimental device to navigate toward igniting regimes through all the foreseeable instabilities and factors that degrade confinement. One of these parameters that can be assumed to measure the maximum attainable value of $n_o \tau_E$, on the basis of present day knowledge, is the confining strength $F_S = I_p B_p$ that we have mentioned already. Here we notice that

$$F_s = I_p^2 / a^2$$

as $B_p \propto I_p / a$, a being the mean radius of the plasma column. By now the high field-technologies have been developed for compact magnets that can confine and produce the highest plasma currents. Since the relevant values of a are relatively small, this would indicate that the compact line of experiments have the best possible intrinsic characteristics in order to achieve ignition conditions.

An important point to be added in this connection is that ignition is not achieved through a sequence of steady states, but through transients that can be exploited to reach the desired conditions. Indeed the present

theoretical knowledge of the behaviour of magnetically confined plasmas does not allow us to predict how the plasma will reach ignition. Two of the most crucial processes determining how ignition can be achieved are the possible onset of oscillations of the central part of the plasma column induced either by the peaked distribution of the α -particle heating or directly by the mode resonant interaction with these particles. Compact ignition experiments can be designed to attain ignition with relatively low values of β_p , which expresses the ratio between the plasma pressure and the energy density of the poloidal magnetic field, so that the threshold for the hard onset of these modes can be avoided to the extent that they are driven by the plasma pressure gradient. In addition, since the design of these experiments include high values of the plasma current I_p , another possibility is to decrease the plasma current to the point where the region that is affected by the instability ($q < 1$) is so reduced that it is irrelevant.

As a final point, it is worth noting that the Ignitor project will bring about a number of beneficial developments, both scientific and technological. In this context it is important to recall that the development of a free electron laser in the wavelength range around half a millimeter, which is of general interest for the physics community at the present time, would provide a convenient tool for heating electrons in a high density, high field configuration. This would allow us to reach ignition conditions at lower temperatures and higher densities or, in a D-He³ reactor, to avoid the use of tritium at the beginning of the discharge to increase the reactivity of the plasma.

Table 1. Main design parameters of the Ignitor Ω experiment.

Major radius $R_o = 110.5$ cm
Plasma cross section $a \times b = 40 \times 72.5$ cm²
Aspect ratio $R_o/a = 2.75$
Plasma current $I_p = 11.25$ megampere
Poloidal field $B_p = 40$ kG
Strength parameter $I_p B_p = 45$ megampere-tesla
Average plasma current density $\langle J_{||} \rangle = 1234$ A/cm²
Toroidal field at the magnetic axis $B_o = 134.6$ kG
Technical safety factor $q_E = 1.57$

Table 2. Characteristics parameters of an experimental D-He³ reactor of the Candor type. The name has been chosen to stress that such a reactor is almost completely neutron free.

Major ratio $R_o = 165$ cm
Plasma cross section $a \times b = 55 \times 100$ cm²
Aspect ratio $R_o/a = 3$
Plasma current $I_p = 13.5$ megampere
Poloidal field $B_p = 35$ kG
Strength parameter $I_p B_p = 47$ megampere-tesla
Average plasma current density $\langle J_{||} \rangle = 781$ A/cm²
Toroidal field at the magnetic axis $B_o = 130$ kG
Technical safety factor $q_E = 1.6$.

REFERENCES

- (1) B.COPPI, Massachusetts Institute of Technology, R.L.E. Report PRR-75/18. Cambridge, Ma, 1975, and Comments on Plasma Physics and Controlled Fusion 3, 2 (1977) Presented at the Special Session on Tokamak Ignition Experiments, 1976 I.A.E.A. Conference, Berchtesgaden, Germany
- (2) B. COPPI, Physics Scripta T2/2 590 (1982)
- (3) R.J. HAWRYLUK et al., Paper IAEA CN-47/A-I-3 in Plasma Physics and Controlled Nuclear Fusion Research 1986. Publ. IAEA, Vienna 1986 (Proceedings of the IAEA Conference, Kyoto, Japan, 1986)
- (4) B. COPPI, F. PEGORARO, G. LAMPIS, L. PIERONI and S. SEGRE', Massachusetts Institute Technology, RLE Report PRR 75/4 (Cambridge, Ma, 1975)
- (5) N. NIEDERMEYER et al., in Plasma Physics and Controlled Nuclear Fusion Research 1986, Paper I.A.E.A.-CN-47/A-II-5 (Publ. I.A.E.A., Vienna, 1987)
- (6) B. COPPI, Massachusetts Institute of Technology, RLE Report, PTP-87/88 (Cambridge, Ma, 1986).

Volume I - numero 1	CINQUANTA ANNI DI INTERAZIONI DEBOLI: DALLA TEORIA DI FERMI ALLA SCOPERTA DEI BOSONI PESANTI - Marcello Conversi	pag. 1
Volume I - numero 2	EFFECTS OF DIOXINS ON NATURE AND SOCIETY - Opening talk, Sergio P. Ratti	pag. 3
	DIOXIN IN MISSOURI - Armon F. Yanders	pag. 11
	DEMONSTRATION OF INNOVATIVE REMEDIAL ACTION TECHNOLOGIES AT UNITED STATES MILITARY DIOXIN CONTAMINATED SITES - Terry L. Stoddart	pag. 23
	TIMES BEACH DIOXIN RESEARCH FACILITY - Robert J. Schreiber	pag. 41
	E.P.A. RISK ASSESSMENT OF CHLORINATED DIBENZO-P-DIOXIN AND DIBENZOFURANS (CCDs/CDFs) Donald G. Barnes, Patricia Roberts	pag. 51
	RECENT INTERNATIONAL COOPERATION IN EXCHANGE OF INFORMATION ON DIOXIN - Donald G. Barnes	pag. 63
	CHLORACNE AND THE AGENT ORANGE PROBLEM IN THE U.S.A. - Betty Fischmann	pag. 69
Volume II - numero 1	MOTIVAZIONI DEL CONVEGNO - Sergio P. Ratti	pag. 3
	LA CONOSCENZA ATTUALE DELLA INTERAZIONE GRAVITAZIONALE: UN PROBLEMA APERTO - Sergio P. Ratti, Roberto Silvotti	pag. 5
	SVILUPPI RECENTI SULLA CONOSCENZA DELLA COSTANTE DI GRAVITAZIONE UNIVERSALE - A. Grassi, G. Strini	pag. 19
	LIMITI SPERIMENTALI SULLA MISURA DELL'ACCELERAZIONE DI GRAVITA' - R. Cassinis	pag. 31
	CONSEGUENZE SPERIMENTALI DELLA IPOTESI DI ESISTENZA DI UNA QUINTA INTERAZIONE - Fabrizio Massa	pag. 43
	VERIFICA DEL PRINCIPIO DI EQUIVALENZA E FORZE TRA PARTICELLE ELEMENTARI - Bruno Bertotti	pag. 81
Volume II - numero 2	TRANSIZIONE LIQUIDO SOLIDO - Mario Tosi	pag. 3
	EQUAZIONI DI MAXWELL NEL VUOTO ED ELETTRO-DINAMICA QUANTISTICA - E. Zavattini	pag. 27

Volume III - numero 1	METODI DI DILATAZIONE ANALITICA E RISONANZE IN SISTEMI QUANTISTICI NON RELATIVISTICI - Fausto Borgonovi	pag. 1
	CAMPO ELETTRICO ED EMISSIONI DA CARICHE IN UN MEZZO - Michele Spada	pag. 13
	SPETTROSCOPIA VIBRAZIONALE SUPERRETICOLI SEMICONDUTTORI - Luciano Colombo	pag. 29
	SOLITONI IN FISICA NUCLEARE - Marco Radici	pag. 51
	ASPETTI NON LOCALI DEL COMPORTAMENTO QUANTISTICO - Oreste Nicosini	pag. 83
Volume III - numero 2	CARATTERIZZAZIONE OTTICA IN SITU DI FILMS SOTTILI - Alessandra Piaggi	pag. 1
	TRANSIZIONI DI WETTING - Tomaso Bellini	pag. 23
	FORZE A TRE CORPI NEI GAS RARI - Silvia Celi	pag. 49
Volume III - numero 3	FLAVOUR PHYSICS - Luciano Maiani	pag. 1
	THE STANDARD ELECTROWEAK MODEL: PRESENT EXPERIMENTAL STATUS - Pierre Darrulat	pag. 27
	WHY BE EVEN-HANDED? - Martin M. Block	pag. 47
Volume IV - numero 1	LA FISICA DEI COLLIDER - Paolo Bagnaia, Fernanda Pastore	pag. 1